Valley-dependent magnetoresistance in two-dimensional semiconductors

Akihiko Sekine and Allan H. MacDonald

Phys. Rev. B **97**, 201301 — Published 30 May 2018

DOI: 10.1103/PhysRevB.97.201301

Valley-Dependent Magnetoresistance in Two-Dimensional Semiconductors

Akihiko Sekine* and Allan H. MacDonald
Department of Physics, The University of Texas at Austin, Austin, Texas 78712, USA
(Dated: May 16, 2018)

We show theoretically that two-dimensional direct-gap semiconductors with a valley degree of freedom, including monolayer transition-metal dichalcogenides and gapped bilayer graphene, have a longitudinal magnetoconductivity contribution that is odd in valley and odd in the magnetic field applied perpendicular to the system. Using a quantum kinetic theory we show how this valley-dependent magnetoconductivity arises from the interplay between the momentum-space Berry curvature of Bloch electrons, the presence of a magnetic field, and disorder scattering. We discuss how the effect can be measured experimentally and used as a detector of valley polarization.

Introduction.— Studies of magnetotransport in metals have a long standing in condensed matter physics. From the viewpoint of technology the discoveries of giant magnetoresistance[1,2] and tunnel magnetoresistance[3–5] have led to drastic improvements in the performance of magnetic information storage devices. More generally magnetoresistance studies can play an important role in characterizing the electronic structure of solids. For example, Shubnikov–de Haas resistance oscillations are routinely used to measure Fermi surfaces. More recently the existence of three-dimensional (3D) Dirac and Weyl semimetals, which have topologically nontrivial band structures, has been confirmed experimentally[6–11] by measuring a remarkable and characteristic negative longitudinal magnetoresistance property associated with the chiral anomaly[12–15].

This Rapid Communication addresses magnetotransport in 2D semiconductors with more than one valley. Valley has recently attracted greater attention as an observable degree of freedom of electrons in solids[16–18], in part because of the emergence of monolayer transition-metal dichalcogenides (TMDs) and gapped bilayer graphene, both 2D semiconductors in which valence and conduction band extrema occur at the K and K' time-reversal partner Brillouin-zone corner points. When intervalley scattering by disorder or phonons is weak, valley remains an approximate quantum number even beyond the Bloch band approximation. Weak valley relaxation combined with valley-dependent contributions to the conductivity tensor can lead to observable effects analogous to those produced by spin accumulations in conductors with weak spin-orbit scattering. To date, attention has focused mainly on the valley-dependent anomalous Hall effect[19,20], which occurs in the absence of a magnetic field and is related to the broken time-reversal symmetry of the Hamiltonian's projection to a single valley, and to momentum-space Berry phase effects. Given the negative magnetoresistance in 3D Dirac and Weyl semimetals, which also involves valleys related by time-reversal, longitudinal magnetotransport effects should be expected in 2D multi-valley systems. We approach this issue theoretically using a massive Dirac model for 2D multi-valley semiconductors and a recently developed quantum kinetic theory[15,21]. We find that the longitudinal magnetoconductivity has a contribution that is odd in valley and odd in perpendicular magnetic field. Our theoretical predictions can be tested by observing a change from quadratic to linear magnetoresistance in systems in which a finite valley polarization is induced by optical pumping or valley injection, as schematically illustrated in Fig. 1.

Magnetotransport theory.— The transport theory we employ is valid in the low magnetic field regime where Landau quantization can be neglected and enables us to systematically compute the conductivity tensor in the presence of disorder in arbitrary spatial dimensions. It is based on a quantum kinetic equation that accounts for disorder, and for electric $\boldsymbol{E}$ and magnetic $\boldsymbol{B}$ fields[15,22]:

$$\frac{\partial\langle\rho\rangle}{\partial t}+\frac{i}{\hbar}[\mathcal{H}_0,\langle\rho\rangle]+K(\langle\rho\rangle)=D_E(\langle\rho\rangle)+D_B(\langle\rho\rangle), \tag{1}$$

where $\langle\rho\rangle$ is the impurity-averaged Bloch-electron density matrix, $\mathcal{H}_0$ is the unperturbed Bloch Hamiltonian, $K(\langle\rho\rangle)$ is a disorder contribution discussed further below, and $D_E(\langle\rho\rangle)$ and $D_B(\langle\rho\rangle)$ are the electric and magnetic driving terms:

$$\begin{aligned} D_E(\langle\rho\rangle) &= \frac{e\boldsymbol{E}}{\hbar}\cdot\frac{D\langle\rho\rangle}{D\boldsymbol{k}}, \\ D_B(\langle\rho\rangle) &= \frac{e}{2\hbar^2}\left\{\left(\frac{D\mathcal{H}_0}{D\boldsymbol{k}}\times\boldsymbol{B}\right)\cdot\frac{D\langle\rho\rangle}{D\boldsymbol{k}}\right\}. \end{aligned} \tag{2}$$

Here, $e>0$, $\boldsymbol{k}$ is the crystal wave-vector, $\{\boldsymbol{a}\cdot\boldsymbol{b}\}=\boldsymbol{a}\cdot\boldsymbol{b}+\boldsymbol{b}\cdot\boldsymbol{a}$ (with $\boldsymbol{a}$ and $\boldsymbol{b}$ being vectors) is a symmetrized operator product, and we have introduced a covariant derivative notation for the wave-vector dependence of the matrices X $(=\langle\rho\rangle,\mathcal{H}_0)$

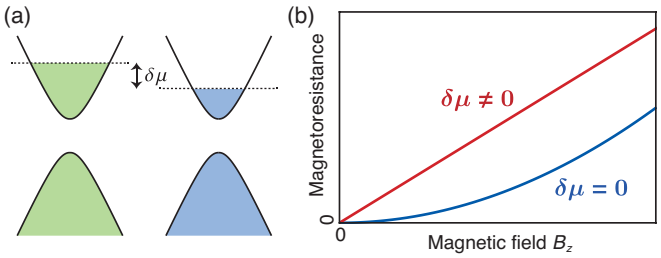

FIG. 1. (a) Schematic illustration of valley polarization due to a chemical potential difference $\delta\mu$ between two valleys in systems with weak intervalley scattering. (b) Schematic of the magnetic-field dependence of the low-magnetic-field magnetoresistance. The magnetoresistance is predicted to have a linear dependence on B_z when $\delta\mu\neq 0$, and a quadratic dependence on B_z when $\delta\mu=0$.

expressed in an eigenstate representation:

$$\frac{DX}{D\boldsymbol{k}} = \frac{\partial X}{\partial \boldsymbol{k}} - i[\mathcal{R}_{\boldsymbol{k}}, X], \tag{3}$$

where $\mathcal{R}_{\boldsymbol{k}} = \sum_{\alpha=x,y,z} \mathcal{R}_{\boldsymbol{k},\alpha} \boldsymbol{e}_\alpha$, and $[\mathcal{R}_{\boldsymbol{k},\alpha}]^{mn} = i\langle u^m_{\boldsymbol{k}} | \partial_{k_\alpha} u^n_{\boldsymbol{k}} \rangle$ is a generalized Berry connection of Bloch electrons.

The steady-state linear response of the density matrix to an electric field can be expressed as a formal expansion in powers of the magnetic field strength B[15,23]: $\langle\rho\rangle = (1 - \mathcal{L}^{-1}D_B)^{-1}\mathcal{L}^{-1}D_E(\langle\rho_0\rangle + \langle\Xi_B\rangle) \equiv \langle\rho_E\rangle + \sum_{N\geq 1}\langle\rho_{B,N}\rangle$, where $\langle\rho_E\rangle = \mathcal{L}^{-1}D_E(\langle\rho_0\rangle)$, $\langle\rho_{B,N}\rangle = (\mathcal{L}^{-1}D_B)^N\mathcal{L}^{-1}D_E(\langle\rho_0\rangle) + (\mathcal{L}^{-1}D_B)^{N-1}\mathcal{L}^{-1}D_E(\langle\Xi_B\rangle)$, and we have defined the Liouvillian operator $\mathcal{L} \equiv P + K$ with $P\langle\rho\rangle \equiv (i/\hbar)[\mathcal{H}_0, \langle\rho\rangle]$. In this expansion $\langle\rho_0\rangle$ is the Fermi-Dirac equilibrium density matrix in the absence of both fields, and $\langle\Xi_B\rangle$ is the equilibrium density matrix in the absence of an electric field. $\langle\Xi_B\rangle$ accounts for the Berry phase correction to the density of states implied by semiclassical wave-packet dynamics[24].

Throughout this Rapid Communication, we work in the eigenstate basis for the various contributions to the steady-state density matrix, and decompose $\langle\rho_{B,N}\rangle$ into its band-diagonal part $\langle n_{B,N}\rangle + \langle\xi_{B,N}\rangle$, and its band-off-diagonal part $\langle S_{B,N}\rangle$. We adopt a relaxation time approximation for the disorder scattering that influences the diagonal part of $\langle\rho_{B,N}\rangle$:

$$\begin{aligned}\langle n_{B,N}\rangle^{mm}_{\boldsymbol{k}} &= \tau_m[D_B(\langle\rho_{B,N-1}\rangle)]^{mm}_{\boldsymbol{k}},\\ \langle\xi_{B,N}\rangle^{mm}_{\boldsymbol{k}} &= \frac{e}{\hbar}\boldsymbol{B}\cdot\boldsymbol{\Omega}^m_{\boldsymbol{k}}\langle n_{B,N-1}\rangle^{mm}_{\boldsymbol{k}},\end{aligned} \tag{4}$$

where $N \geq 1$, $\langle\rho_{B,0}\rangle = \langle\rho_E\rangle$, $\langle n_{B,0}\rangle = 2\langle n_E\rangle$, and τ_m and $\boldsymbol{\Omega}^m_{\boldsymbol{k}}$ are respectively the scattering time and the Berry curvature vector for band m. We also have $\langle\Xi_B\rangle^{mm}_{\boldsymbol{k}} = (e/\hbar)\boldsymbol{B}\cdot\boldsymbol{\Omega}^m_{\boldsymbol{k}}\langle\rho_0\rangle^{mm}_{\boldsymbol{k}}$. In Eq. (4), $\langle n_{B,N}\rangle$ is the extrinsic (Lorentz force) contribution, while $\langle\xi_{B,N}\rangle$ is the intrinsic (Berry phase) contribution. The band off-diagonal part is given by[15]

$$\langle S_{B,N}\rangle^{mm'}_{\boldsymbol{k}} = \frac{\hbar}{i}\frac{[D_B(\langle\rho_{B,N-1}\rangle)]^{mm'}_{\boldsymbol{k}} - [J(\langle n_{B,N}\rangle)]^{mm'}_{\boldsymbol{k}}}{\varepsilon^m_{\boldsymbol{k}} - \varepsilon^{m'}_{\boldsymbol{k}}}, \tag{5}$$

where $m \neq m'$ and $\varepsilon^m_{\boldsymbol{k}}$ is the energy eigenvalue of band m. In Eq. (5) the term proportional to $D_B(\langle\rho_{B,N-1}\rangle)$ is purely a band-structure property expressed in terms of the Berry connection, whereas the term proportional to $J(\langle n_{B,N}\rangle)$ is a disorder-dependent Fermi-surface response corresponding to a vertex correction in the ladder-diagram approximation[15,21]. The explicit form of $J(\langle n_{B,N}\rangle)$ will be given later.

Massive Dirac model.— We consider 2D semiconductors with broken inversion symmetry, like monolayer TMDs, that have two low-energy valleys related by time-reversal. The low-energy effective Hamiltonians in these systems normally have the massive Dirac form[16,19,25]

$$\mathcal{H}_{\tau_z}(\boldsymbol{k}) = v_F(\tau_z k_x\sigma_x + k_y\sigma_y) + m\sigma_z. \tag{6}$$

(As we discuss briefly later, gated bilayer graphene is an exception.) In Eq. (6) $\tau_z = \pm 1$ distinguishes the two valleys, v_F is the Fermi velocity, $2m$ is the band gap, and the Pauli matrices σ_i act in the space of the retained conduction and valence bands. The eigenvalues of the Hamiltonian (6) are $\pm\varepsilon_{\boldsymbol{k}} = \pm\sqrt{v_F^2(k_x^2 + k_y^2) + m^2}$ with the eigenfunctions $|u^\pm_{\boldsymbol{k}}(\tau_z)\rangle$. From Eq. (3), we see that the wavevector dependence of the eigenfunctions $|u^\pm_{\boldsymbol{k}}(\tau_z)\rangle$ plays an important role in our transport theory. In the eigenstate basis the Berry connection vector $[\mathcal{R}^{\tau_z}_{\boldsymbol{k},\alpha}]^{mn} = i\langle u^m_{\boldsymbol{k}}(\tau_z)|\partial_{k_\alpha}u^n_{\boldsymbol{k}}(\tau_z)\rangle$ with $m, n = \pm$ has the explicit form

$$\begin{aligned}\mathcal{R}^{\tau_z}_{\boldsymbol{k},x} &= \frac{1}{2k}\tau_z\sin\theta - \tilde{\sigma}_z\frac{m}{2k\varepsilon_{\boldsymbol{k}}}\tau_z\sin\theta - \tilde{\sigma}_y\frac{v_F m}{2\varepsilon^2_{\boldsymbol{k}}}\cos\theta\\ &\quad - \tilde{\sigma}_x\frac{v_F}{2\varepsilon_{\boldsymbol{k}}}\tau_z\sin\theta,\\ \mathcal{R}^{\tau_z}_{\boldsymbol{k},y} &= -\frac{1}{2k}\tau_z\cos\theta + \tilde{\sigma}_z\frac{m}{2k\varepsilon_{\boldsymbol{k}}}\tau_z\cos\theta - \tilde{\sigma}_y\frac{v_F m}{2\varepsilon^2_{\boldsymbol{k}}}\sin\theta\\ &\quad + \tilde{\sigma}_x\frac{v_F}{2\varepsilon_{\boldsymbol{k}}}\tau_z\cos\theta,\end{aligned} \tag{7}$$

where $e^{\pm i\theta} = (k_x \pm ik_y)/k$, $k = \sqrt{k_x^2 + k_y^2}$, and $\tilde{\sigma}_\alpha$ is a Pauli matrix that acts in the eigenstate basis. Also, the Berry curvature takes the form $[\Omega^{\tau_z}_{\boldsymbol{k},z}]^\pm = i\langle\partial_{k_x}u^\pm_{\boldsymbol{k}}(\tau_z)|\partial_{k_y}u^\pm_{\boldsymbol{k}}(\tau_z)\rangle - i\langle\partial_{k_y}u^\pm_{\boldsymbol{k}}(\tau_z)|\partial_{k_x}u^\pm_{\boldsymbol{k}}(\tau_z)\rangle = \mp\tau_z v_F^2 m/(2\varepsilon^3_{\boldsymbol{k}})$.

Valley-dependent longitudinal magnetoconductivity.— We apply our magnetotransport theory to the 2D systems described by Eq. (6) with a static magnetic field $\boldsymbol{B} = (0, 0, B_z)$ applied perpendicular to the system. For the moment we neglect the vertex correction, i.e., the contribution proportional to J in Eq. (5). Without loss of generality we may consider an electron-doped case with positive chemical potential μ. Our goal is to compute the xx-component of the magnetoconductivity tensor using

$$\sigma^{(N)}_{\mu\nu}(B_z) = \mathrm{Tr}\left[(-e)v_\mu\langle\rho_{B,N}\rangle\right]/E_\nu. \tag{8}$$

In the eigenstate basis the velocity operator reads $v_x = v_F(\tilde{\sigma}_z\frac{v_F k}{\varepsilon_{\boldsymbol{k}}}\cos\theta + \tilde{\sigma}_y\tau_z\sin\theta - \tilde{\sigma}_x\frac{m}{\varepsilon_{\boldsymbol{k}}}\cos\theta)$.

We first evaluate the magnetoconductivity contributions proportional to odd powers of B_z for $\mu > m$ in the conduction band. The linear magnetoconductivity $\sigma^{(1)}_{xx}(B_z)$ is determined by the density matrix $\langle\rho_{B,1}\rangle = \mathcal{L}^{-1}D_B(\langle\rho_E\rangle) + \mathcal{L}^{-1}D_E(\langle\Xi_B\rangle)$. We find that[26]

$$\begin{aligned}\sigma^{(1)}_{xx}(B_z) &= \tau_z\frac{e^2B_z}{E_x}\int[d\boldsymbol{k}]\left[\frac{v_F^2 m}{2\varepsilon^2_{\boldsymbol{k}}}\frac{\partial}{\partial k_x} + \frac{v_F^4 m k_x}{\varepsilon^4_{\boldsymbol{k}}}\right]\langle n_E\rangle^{++}_{\boldsymbol{k}}\\ &\equiv \tau_z\frac{e^3}{\hbar}B_z v_F^2 C_1(\mu, m)\tau_{\mathrm{tr}},\end{aligned} \tag{9}$$

where $[d\boldsymbol{k}] \equiv \frac{d^2k}{(2\pi)^2}$, $\langle n_E\rangle^{++}_{\boldsymbol{k}} = \tau_{\mathrm{tr}}(eE_x/\hbar)\partial f_0(\varepsilon_{\boldsymbol{k}})/\partial k_x$, $f_0(\varepsilon_{\boldsymbol{k}})$ is the Fermi-Dirac distribution function, τ_{tr} is the intravalley scattering time, and $C_1(\mu, m) < 0$ is evaluated by performing a numerical integration. The two terms in square brackets of Eq. (9) acting on the extrinsic response $\langle n_E\rangle$ arise respectively from the off-diagonal intrinsic contribution $\langle S_{B,1}\rangle$ and the diagonal intrinsic contribution $\langle\xi_{B,1}\rangle$. In Fig. 2 we show the μ and m dependences of $\sigma^{(1)}_{xx}(B_z)$. It should be noted here that, as seen from Fig. 2(b), $\sigma^{(1)}_{xx}(B_z)$ is significantly enhanced in a smaller gap system. Similarly, we find the cubic magnetocon-

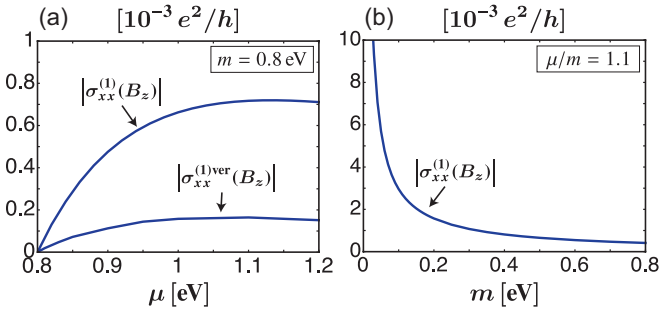

FIG. 2. (a) Chemical potential μ dependence of $\sigma_{xx}^{(1)}(B_z)$ [Eq. (9)] and $\sigma_{xx}^{(1)\mathrm{ver}}(B_z)$ [Eq. (14)] for $m = 0.8$ eV. Both $\sigma_{xx}^{(1)}(B_z)$ and $\sigma_{xx}^{(1)\mathrm{ver}}(B_z)$ are proportional to m/μ^2 in the case of $\mu \gg m$ and thus approach zero in the limit $\mu \gg m$. (b) Band gap m dependence of $\sigma_{xx}^{(1)}(B_z)$ for $\mu/m = 1.1$. In both (a) and (b), we set $B_z = 0.1$ T, $v_F = 3\,\mathrm{eV}\cdot\text{Å}$, $\tau_{\mathrm{tr}} = 0.1$ ps, and $T = 5$ meV.

ductivity obtained from $\langle\rho_{B,3}\rangle$[26]

$$\sigma_{xx}^{(3)}(B_z) = \frac{8}{3}\tau_z\frac{e^2B_z}{E_x}\int[d\boldsymbol{k}]\left[\frac{v_F^2 m}{2\varepsilon_{\boldsymbol{k}}^2}\frac{\partial}{\partial k_x} + \frac{v_F^4 m k_x}{2\varepsilon_{\boldsymbol{k}}^4}\right]\langle n_{B,2}\rangle_{\boldsymbol{k}}^{++}$$
$$\equiv \tau_z\frac{e^5}{\hbar}B_z^3 v_F^6 C_3(\mu,m)\tau_{\mathrm{tr}}^3, \tag{10}$$

where $\langle n_{B,2}\rangle_{\boldsymbol{k}}^{++} = (eB_z\tau_{\mathrm{tr}})^2(\frac{\partial\varepsilon_{\boldsymbol{k}}}{\partial k_y}\frac{\partial}{\partial k_x} - \frac{\partial\varepsilon_{\boldsymbol{k}}}{\partial k_x}\frac{\partial}{\partial k_y})^2\langle n_E\rangle_{\boldsymbol{k}}^{++}$, and $C_3(\mu,m) > 0$. In the case of $\mu \gg m$, we find that $C_3(\mu,m) \propto m/\mu^4$. For the material parameters used in Fig. 2(a), $|\sigma_{xx}^{(3)}(B_z)/\sigma_{xx}^{(1)}(B_z)| \sim 10^{-3}(B_z\,[\mathrm{T}])^2$. The two terms in square brackets of Eq. (10) acting on the extrinsic response $\langle n_{B,2}\rangle$ arise respectively from the off-diagonal intrinsic contribution $\langle S_{B,3}\rangle$ and the diagonal intrinsic contribution $\langle\xi_{B,3}\rangle$. There are no valley-independent contributions to the linear and cubic magnetoconductivities, as required by time-reversal symmetry. Higher-order odd-power terms have the general form

$$\sigma_{xx}^{(N)}(B_z) = \tau_z\frac{e^{N+2}}{\hbar}B_z^N v_F^{2N} C_N(\mu,m)\tau_{\mathrm{tr}}^N, \tag{11}$$

where $N = 5, 7, 9\cdots$ is an odd integer and $C_N(\mu,m)$ has the dimension of $[\mathrm{Energy}]^{-N}$.

Next, we consider the magnetoconductivity contributions proportional to even powers of B_z, which cannot be valley dependent due to time-reversal symmetry[27]. We find that the quadratic magnetoconductivity obtained from $\langle\rho_{B,2}\rangle$ is dominated by the Lorentz-force contribution

$$\sigma_{xx}^{(2)}(B_z)$$
$$\approx -\frac{e^3B_z^2\tau_{\mathrm{tr}}^2}{E_x}\int[d\boldsymbol{k}]\frac{v_F^2 k_x}{\varepsilon_{\boldsymbol{k}}}\left(\frac{\partial\varepsilon_{\boldsymbol{k}}}{\partial k_y}\frac{\partial}{\partial k_x} - \frac{\partial\varepsilon_{\boldsymbol{k}}}{\partial k_x}\frac{\partial}{\partial k_y}\right)^2\langle n_E\rangle_{\boldsymbol{k}}^{++}$$
$$= -\sigma_{xx}^{(0)}(\omega_c\tau_{\mathrm{tr}})^2, \tag{12}$$

where $\sigma_{xx}^{(0)} = (-e/E_x)\int[d\boldsymbol{k}](v_F^2 k_x/\varepsilon_{\boldsymbol{k}})\langle n_E\rangle_{\boldsymbol{k}}^{++}$ is the Drude conductivity and $\omega_c = eB_z v_F^2/\mu$ is the cyclotron frequency. Intrinsic contributions to the quadratic magnetoconductivity are not zero, but they are suppressed by $\sim 1/(\mu\tau_{\mathrm{tr}})^2 \ll 1$ compared to the conventional contribution in Eq. (12)[26].

Vertex corrections.— From Eq. (5) the vertex correction contribution to the density matrix linear in B_z is given by $\langle S'_{B,1}\rangle_{\boldsymbol{k}}^{mm''} \equiv i\hbar[J(\langle n_{B,1}\rangle)]_{\boldsymbol{k}}^{mm''}/(\varepsilon_{\boldsymbol{k}}^m - \varepsilon_{\boldsymbol{k}}^{m''})$, where[21]

$$[J(\langle n\rangle)]_{\boldsymbol{k}}^{mm''} = \frac{\pi}{\hbar}\sum_{m'\boldsymbol{k}'}\langle U_{\boldsymbol{k}\boldsymbol{k}'}^{mm'}U_{\boldsymbol{k}'\boldsymbol{k}}^{m'm''}\rangle\Big[(n_{\boldsymbol{k}}^m - n_{\boldsymbol{k}'}^{m'})\delta(\varepsilon_{\boldsymbol{k}}^m - \varepsilon_{\boldsymbol{k}'}^{m'})$$
$$+ (n_{\boldsymbol{k}}^{m''} - n_{\boldsymbol{k}'}^{m'})\delta(\varepsilon_{\boldsymbol{k}}^{m''} - \varepsilon_{\boldsymbol{k}'}^{m'})\Big]. \tag{13}$$

Here, $m \neq m''$ and $\langle n\rangle = \mathrm{diag}[n_{\boldsymbol{k}}^m]$ is an arbitrary band-diagonal density matrix. We assume short-range disorder of the form $U(\boldsymbol{r}) = U_0\sum_i\delta(\boldsymbol{r} - \boldsymbol{r}_i)$ with $\langle U(\boldsymbol{r})U(\boldsymbol{r}')\rangle = n_{\mathrm{imp}}U_0^2\,\delta(\boldsymbol{r} - \boldsymbol{r}')$, where n_{imp} is the impurity density. After a lengthy calculation[26], we find the vertex correction to the linear magnetoconductivity

$$\sigma_{xx}^{(1)\mathrm{ver}}(B_z) = \mathrm{Tr}\left[(-e)v_x\langle S'_{B,1}\rangle\right]/E_x$$
$$= \tau_z\frac{e^3}{\hbar}B_z v_F^2 C_1^{\mathrm{ver}}(\mu,m)\tau_{\mathrm{tr}}, \tag{14}$$

where $C_1^{\mathrm{ver}}(\mu,m) < 0$. This means that the vertex correction enhances the valley-dependent linear magnetoconductivity [see Fig. 2(a)]. This contrasts with its well-known influence on the the spin Hall[28] and anomalous Hall[29] conductivities in certain Rashba models, i.e., the suppression of these conductivities by the vertex correction. Here, we note that usual golden-rule intraband scattering rates proportional to $\langle U_{\boldsymbol{k}\boldsymbol{k}'}^{++}U_{\boldsymbol{k}'\boldsymbol{k}}^{++}\rangle$ are not valley dependent. Nonzero contributions to Eq. (14) require interband scattering matrix elements like $\langle U_{\boldsymbol{k}\boldsymbol{k}'}^{++}U_{\boldsymbol{k}'\boldsymbol{k}}^{+-}\rangle$, which are valley dependent. The vertex correction is valley dependent because it is due to interband coherence induced by the magnetic field.

Discussion.— A longitudinal total magnetoconductivity proportional to odd powers of magnetic field can occur only in systems with broken time-reversal symmetry[30,31]. In monolayer TMDs and gated bilayer graphene, spatial inversion symmetry is broken but time-reversal symmetry is retained. The valley-dependent magnetoconductivity contributes to transport only in the presence of a finite valley polarization, for example one due to a chemical potential difference between the two valleys, that explicitly breaks time-reversal symmetry. Valley polarization in TMDs can be realized by applying circularly polarized light[16,32–34] to generate an excess population of carriers in one valley. When intravalley scattering is much stronger than intervalley scattering, equilibration will occur within valleys to establish valley-dependent chemical potentials. This approach has been used previously to measure the valley Hall effect[20], and is the most direct way to measure the valley-dependent magnetoconductivity derived in this Rapid Communication. In discussing the results of such a measurement below, we assume that the contribution to transport from photo-generated holes is negligible.

Including terms up to order of B_z^2 and allowing for a chemical potential difference between valleys, the total magnetoconductivity of a two-valley system reads

$$\sigma_{xx}^B(\mu_1,\mu_2) = \frac{e^3}{\hbar}B_z v_F^2[C_1^{\mathrm{tot}}(\mu_1,m) - C_1^{\mathrm{tot}}(\mu_2,m)]\tau_{\mathrm{tr}}$$
$$- \sigma_{xx}^{(0)}(\mu_1)(\omega_{c1}\tau_{\mathrm{tr}})^2 - \sigma_{xx}^{(0)}(\mu_2)(\omega_{c2}\tau_{\mathrm{tr}})^2, \tag{15}$$

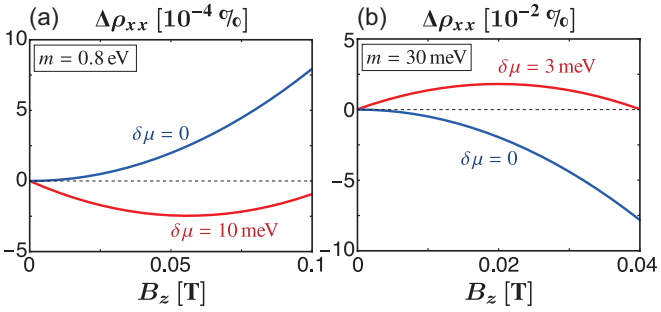

FIG. 3. (a) Valley polarization $\delta\mu$ dependence of the magnetoresistance $\Delta\rho_{xx}(B_z, \delta\mu)$ [Eq. (16)] in the case of $|\sigma^{(0)}_{xx}/\sigma^{(0)}_{xy}| \gg 1$ for $m = 0.8\,\mathrm{eV}$, corresponding to the typical gap of monolayer TMDs. We used $\mu_1 = \mu_2 = 0.82\,\mathrm{eV}$ for the $\delta\mu = 0$ case, and $\mu_1 = 0.83\,\mathrm{eV}$ and $\mu_2 = 0.82\,\mathrm{eV}$ for the $\delta\mu \neq 0$ case. (b) $\Delta\rho_{xx}(B_z, \delta\mu)$ in the case of $|\sigma^{(0)}_{xx}/\sigma^{(0)}_{xy}| \ll 1$ for $m = 30\,\mathrm{meV}$, corresponding to low-carrier-density gated bilayer graphene. We used $\mu_1 = \mu_2 = 33\,\mathrm{meV}$ for the $\delta\mu = 0$ case, and $\mu_1 = 36\,\mathrm{meV}$ and $\mu_2 = 33\,\mathrm{meV}$ for the $\delta\mu \neq 0$ case. Note that the magnetoresistance effect is much stronger in a smaller gap system. In both (a) and (b), we set $v_F = 3\,\mathrm{eV}\cdot\mathrm{\AA}$, $\tau_{\mathrm{tr}} = 0.1\,\mathrm{ps}$, and $T = 5\,\mathrm{meV}$.

where μ_i $(i = 1, 2)$ is the chemical potential of valley i, $C_1^{\mathrm{tot}}(\mu_i, m) = C_1(\mu_i, m) + C_1^{\mathrm{ver}}(\mu_i, m)$, and $\omega_{ci} = eB_z v_F^2/\mu_i$. In the low-field limit $\sigma^B_{xx} \propto B_z$ when $\delta\mu = \mu_1 - \mu_2 \neq 0$, while $\sigma^B_{xx} \propto B_z^2$ when $\delta\mu = 0$. The resistivity is defined by $\rho_{xx}(B_z) = \sigma_{xx}/(\sigma_{xx}^2 + \sigma_{xy}^2)$ with $\sigma_{\mu\nu} \equiv \sigma^{(0)}_{\mu\nu} + \sigma^B_{\mu\nu}$. It follows that the low-field magnetoresistance

$$\Delta\rho_{xx} \equiv \frac{\rho_{xx}(B_z) - \rho_{xx}(0)}{\rho_{xx}(0)} \approx \mp \frac{\sigma^B_{xx}(\mu_1, \mu_2)}{\sigma^{(0)}_{xx}(\mu_1) + \sigma^{(0)}_{xx}(\mu_2)}. \qquad (16)$$

Here, the $-$ $(+)$ sign applies in the $|\sigma^{(0)}_{xx}/\sigma^{(0)}_{xy}| \gg 1$ case ($|\sigma^{(0)}_{xx}/\sigma^{(0)}_{xy}| \ll 1$ case)[35]. Obviously the Drude conductivity $\sigma^{(0)}_{xx}$ is not valley dependent. Thus the change in magnetic-field dependence from B_z^2 to B_z when illuminated by circularly polarized light, illustrated schematically in Fig. 1, should be readily observable[36]. Interestingly, we can always make the $\delta\mu \neq 0$ magnetoresistance in the low-field limit opposite in sign to the $\delta\mu = 0$ magnetoresistance by changing the sense of circular light polarization, as illustrated in Fig. 3.

The magnetoresistance effects discussed in this Rapid Communication are much stronger, for a given Fermi velocity, in Dirac models with a smaller gap, and we expect them to be much more easily observed experimentally in bilayer graphene systems than in monolayer TMDs. Bilayer graphene is described by a generalized Dirac model with chirality $J = 2$ rather than $J = 1$, and has quadratic dispersion in the absence of a gap[37]. For a given gap the size of the magnetoresistance effect in bilayer graphene will exceed the $J = 1$ model values plotted in Fig. 3(b).

A valley-dependent conductivity can lead to valley accumulation in the absence of optical valley pumping when an inhomogeneity is present along the current path, for example a variation in carrier density induced by external gates. Because valley dependence is largest in a relative sense when the carrier density is small (i.e., when the Fermi energy μ is only slightly larger than the gap m), the current partitioning between valleys corresponding to equal electro-chemical potential gradients changes across interfaces at which the carrier density changes. If intervalley scattering is weak, valley accumulation will persist within a valley relaxation length of any such interface, and should be detectable via Kerr microscopy[38].

Summary.— To summarize, we have theoretically demonstrated the existence of a valley-dependent longitudinal magnetoconductivity in 2D semiconductors with a valley degree of freedom. The effect arises from the interplay between the momentum-space Berry curvature of Bloch electrons, the presence of a magnetic field, and disorder scattering. Our prediction can be verified by measuring the influence of circularly-polarized light illumination on magnetoresistance in the low-field limit. Because the magnetoresistance is proportional to valley polarization it can be used as a valley detector. We predict that these magnetoresistance effects will be significantly enhanced in bilayer graphene samples with small gaps and small carrier densities.

We thank H. Chen and D. Culcer for valuable discussions. This work was supported by the Department of Energy, Office of Basic Energy Sciences under Contract No. DE-FG02-ER45958 and by the Welch foundation under Grant No. TBF1473. A.S. is supported by the JSPS Overseas Research Fellowship.

* Present address: Center for Emergent Matter Science, RIKEN, Wako, Saitama 351-0198, Japan. akihiko.sekine@riken.jp

[1] M. N. Baibich, J. M. Broto, A. Fert, F. Nguyen Van Dau, F. Petroff, P. Etienne, G. Creuzet, A. Friederich, and J. Chazelas, Phys. Rev. Lett. **61**, 2472 (1988).
[2] G. Binasch, P. Grünberg, F. Saurenbach, and W. Zinn, Phys. Rev. B **39**, 4828(R) (1989).
[3] M. Julliere, Phys. Lett. **54A**, 225 (1975).
[4] T. Miyazaki and N. Tezuka, J. Magn. Magn. Mater. **139**, L231 (1995).
[5] J. S. Moodera, L. R. Kinder, T. M. Wong, and R. Meservey, Phys. Rev. Lett. **74**, 3273 (1995).
[6] J. Xiong, S. K. Kushwaha, T. Liang, J. W. Krizan, M. Hirschberger, W. Wang, R. J. Cava, and N. P. Ong, Science **350**, 413 (2015).
[7] C.-Z. Li, L.-X. Wang, H. Liu, J. Wang, Z.-M. Liao, and D.-P. Yu, Nat. Commun. **6**, 10137 (2015).
[8] X. Huang, L. Zhao, Y. Long, P. Wang, D. Chen, Z. Yang, H. Liang, M. Xue, H. Weng, Z. Fang, X. Dai, and G. Chen, Phys. Rev. X **5**, 031023 (2015).
[9] H. Li, H. He, H.-Z. Lu, H. Zhang, H. Liu, R. Ma, Z. Fan, S.-Q. Shen, and J. Wang, Nat. Commun. **7**, 10301 (2016).
[10] Q. Li, D. E. Kharzeev, C. Zhang, Y. Huang, I. Pletikosi, A. V. Fedorov, R. D. Zhong, J. A. Schneeloch, G. D. Gu, and T. Valla, Nat. Phys. **12**, 550 (2016).
[11] F. Arnold, C. Shekhar, S.-C. Wu, Y. Sun, R. D. dos Reis, N. Ku-

mar, M. Naumann, M. O. Ajeesh, M. Schmidt, A. G. Grushin, J. H. Bardarson, M. Baenitz, D. Sokolov, H. Borrmann, M. Nicklas, C. Felser, E. Hassinger, and B. Yan, Nat. Commun. **7**, 11615 (2016).
[12] D. T. Son and B. Z. Spivak, Phys. Rev. B **88**, 104412 (2013).
[13] A. A. Burkov, Phys. Rev. Lett. **113**, 247203 (2014).
[14] B. Z. Spivak and A. V. Andreev, Phys. Rev. B **93**, 085107 (2016).
[15] A. Sekine, D. Culcer, and A. H. MacDonald, Phys. Rev. B **96**, 235134 (2017).
[16] D. Xiao, G.-B. Liu, W. Feng, X. Xu, and W. Yao, Phys. Rev. Lett. **108**, 196802 (2012).
[17] X. Xu, W. Yao, D. Xiao, and T. F. Heinz, Nat. Phys. **10**, 343 (2014).
[18] K. F. Mak and J. Shan, Nat. Photonics **10**, 216 (2016).
[19] D. Xiao, W. Yao, and Q. Niu, Phys. Rev. Lett. **99**, 236809 (2007).
[20] K. F. Mak, K. L. McGill, J. Park, and P. L. McEuen, Science **344**, 1489 (2014).
[21] D. Culcer, A. Sekine, and A. H. MacDonald, Phys. Rev. B **96**, 035106 (2017).
[22] The quantum kinetic equation (1) reduces to the usual semiclassical Boltzmann equation in spin-independent single-band systems, since the covariant derivatives reduce to simple derivatives in such systems. In this work we treat disorder in the Born approximation, although we can in principle go beyond this in our formalism. In the approximation we employ, the results obtained by our quantum kinetic formalism are equivalent to those obtained by the Kubo formalism with vertex corrections included in the ladder-diagram approximation and both band diagonal and band off-diagonal terms taken into account. If only band diagonal terms were retained, our approach would be equivalent to the standard semiclassical Boltzmann theory. One of the advantages of our formalism is that Berry phase and disorder contributions can be incorporated in a unified fashion at each order of electric and magnetic field strengths.
[23] See Supplemental Material for the detailed derivation.
[24] D. Xiao, J. Shi, and Q. Niu, Phys. Rev. Lett. **95**, 137204 (2005).
[25] C.-C. Liu, W. Feng, and Y. Yao, Phys. Rev. Lett. **107**, 076802 (2011).
[26] See Supplemental Material for a detailed calculation of $\sigma_{xx}^{(1)}(B_z)$, $\sigma_{xx}^{(2)}(B_z)$, and $\sigma_{xx}^{(3)}(B_z)$.
[27] Under time reversal valleys change place and the field direction is reversed. The response must be odd in time and odd in field or even in time and even in field.
[28] J. Inoue, G. E.W. Bauer, and L.W. Molenkamp, Phys. Rev. B **70**, 041303 (2004).
[29] J. Inoue, T. Kato, Y. Ishikawa, H. Itoh, G. E. W. Bauer, and L. W. Molenkamp, Phys. Rev. Lett. **97**, 046604 (2006).
[30] L. Onsager, Phys. Rev. **37**, 405 (1931).
[31] H. Chen, Y. Gao, D. Xiao, A. H. MacDonald, and Q. Niu, arXiv:1511.02557.
[32] T. Cao, G. Wang, W. Han, H. Ye, C. Zhu, J. Shi, Q. Niu, P. Tan, E. Wang, B. Liu, and J. Feng, Nat. Commun. **3**, 887 (2012).
[33] H. Zeng, J. Dai, W. Yao, D. Xiao, and X. Cui, Nat. Nanotechnol. **7**, 490 (2012).
[34] K. F. Mak, K. He, J. Shan, and T. F. Heinz, Nat. Nanotechnol. **7**, 494 (2012).
[35] Note that the anomalous Hall conductivity $\sigma_{xy}^{(0)}$ takes the maximum value $\tau_z e^2/2h$ when the system is insulating, i.e., when $\mu_i < m$ in our model. See Supplemental Material for a detailed derivation of $\Delta\rho_{xx}$.
[36] Note that Fig. 1(b) is an enlarged view of the absolute values of the magnetoresistance $\Delta\rho_{xx}$ at the magnetic field scale $B_z \sim 0.01$ T.
[37] H. Min and A. H. MacDonald, Phys. Rev. B **77**, 155416 (2008).
[38] J. Lee, K. F. Mak, and J. Shan, Nat. Nanotechnol. **11**, 421 (2016).